

Thermal-electric domains in metal conductors

A. M. Kadigrobov, A. A. Slutskin, and I. V. Krivosheĭ

Khar'kov State University

(Submitted 17 November 1983; resubmitted 28 May 1984)

Zh. Éksp. Teor. Fiz. **87**, 1314–1329 (October 1984)

We investigate the thermal-electric instability that arises in a metal as a result of Joule heating of the sample when the conductivity of the metal is a monotonically decreasing function of temperature. The structure of the moving thermal-electric domains that arise spontaneously in this situation is studied and the dependence of their parameters on the physical characteristics of the metal is determined. In particular, the speed of the thermal-electric domains is found to be proportional to the thermal emf coefficient of the metal. A classification is made of the possible types of I-V characteristics of the metal in the case of "cyclic" domains, which occur in ring-shaped samples when an electric field is inductively excited in the sample. The existence of turbulent regimes is shown to be possible in principle. Criteria are found for the stability of thermal-electric domains and the boundaries of the stability regions are plotted with sample-length and as the coordinates. An adiabatic approach is developed which makes possible a complete study of the kinetics of small-amplitude thermal-electric domains.

§1. FORMULATION OF PROBLEM

In the physics of semiconductors the Gunn effect¹ is well known. This is the spontaneous appearance of (moving) electric domains that are formed in the region of electric fields \mathcal{E} where the I-V characteristic of a semiconductor is N -shaped. In our paper² we showed that electric-domain instability due to an N -type I-V characteristic is also possible in normal metals (at low temperatures). This effect differs from its semiconductor analog not only by the existence of an N -type I-V characteristic, but also in that the electrical instability in a metal always takes place at very low electric fields under conditions of local electrical neutrality of the sample.

In Ref. 2 two types of mechanisms for the formation of N -type I-V characteristics in a metal were described. Mechanisms of one type obtain under conditions of coherent magnetic breakdown.³ The anomalous sensitivity of the electron dynamics of the magnetic breakdown to weak electric fields is based on this type of mechanism. The other type of mechanism has a macroscopic character: the N -shaped I-V characteristic is caused by the electric current heating the sample to a temperature at which the resistance is mainly determined by the electron-phonon interaction and therefore increases with \mathcal{E} . The resulting "thermal-electric" instability that arises (already observed experimentally⁴⁻⁶) is the subject of this paper. We examine here the structure and dynamics of thermal-electric domains in metal samples that are so thin that nonuniformities in the temperature distribution over their cross section can be neglected.

At a uniform distribution of temperature T along the sample the dependence of T on \mathcal{E} is determined from the heat-balance condition:

$$j\mathcal{E} = d^{-1}q(T), \quad j = \sigma(T)\mathcal{E}, \quad (1)$$

where j is the current along the sample, $\sigma(T)$ is the electrical conductivity at a given temperature, $q(T)$ is the heat flow per unit area of sample surface, and d is a geometric factor equal to the ratio of the cross section to the perimeter of the sam-

ple. From (1) it follows immediately that the differential conductivity $dj/d\mathcal{E}$ is negative if the sample is heated to a temperature where

$$d(\sigma q)/dT < 0. \quad (2)$$

Thus, the basic properties of the physical system we are studying are determined by the behavior of the function $\chi(T) = \sigma(T)q(T)$. In a metal this function, as a rule, is N -shaped¹⁾ (Fig. 1). In such a case, the maximum point T_A of this function (see Fig. 1) is always in the low temperature region where the electron-impurity relaxation time t_{ei} and the electron-phonon relaxation time $t_{ep} \propto T^{-5}$ are of the same order of magnitude. Because the heat outflow $q(T)$ in-

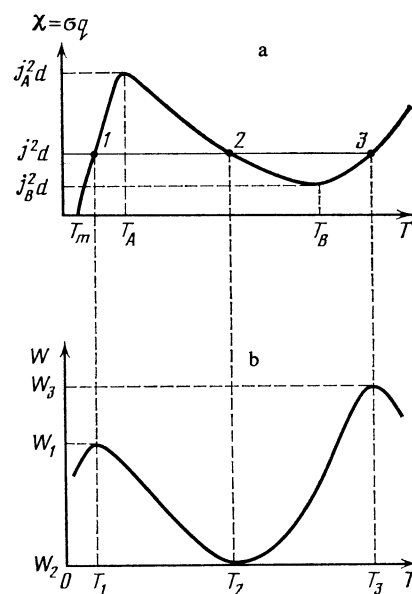


FIG. 1. a) The function $\chi(T) = \sigma(T)q(T)$; b) The potential energy $W(T, j)$. The extrema of the potential energy are located at the points T_1 , T_2 , and T_3 , where $\chi(T) = dj^2$. The initial value of the potential energy is chosen such that $W(T_2, j) = 0$. Here T_m is the temperature of the thermostat and T_A and T_B are the extremal points of $\chi(T)$.

creases slowly with temperature T , the second rising portion of the function $\chi(T)$ is located in the temperature range where the conductivity $\sigma(T)$ approaches asymptotically the function T^{-1} , i.e., the temperature T_B of the minimum of the function $\chi(T)$ is of the order of the Debye temperature T_D of the conductor. For a metal with a resistance ratio $R_{4,2}/R_{273} < 10^{-2}$, the value of T_A is $\sim 10\text{--}30$ K. The heat outflow corresponding to this T_A is $q \sim 10^{-1}$ to 1 W/cm², and the electric field is $\mathcal{E} \sim 10^{-5}\text{--}10^{-6}$ CGS units, which is at least six orders of magnitude less than in semiconductors.¹ Such small values of \mathcal{E} can be produced both in the usual experimental setup (with the sample connected into an electrical circuit with a voltage source), or with a contactless arrangement designed especially for metals. In the latter, the electric field is induced in a short-circuited sample by slow variation of the magnetic flux. As will be seen in the subsequent discussion, the contactless experimental apparatus creates a number of novel physical situations that are not realized in the case of semiconductors.

The entire following treatment pertains to the experimental case where the voltage is specified (thermal-electric domain is unstable if dc is used), i.e., we assume that in the contactless case we can neglect the inductive effect of the sample on the source of the alternating magnetic field, while in the case of a sample that is connected to an external circuit we can neglect the resistance of the circuit compared with that of the sample. Using the known relation (see e.g., Ref. 7) between the electric field $\mathcal{E}(x,t)$ in the sample and the temperature $T(x,t)$, where x is the coordinate along the sample and t is the time, and taking it into account that $T(x,t)$ satisfies the equation of continuity of heat flow from the sources, we obtain the following system of basic equations of the problem:

$$C_v(T) \frac{\partial T}{\partial t} + j(t) T \frac{d\alpha}{dT} \frac{\partial T}{\partial x} - \frac{\partial}{\partial x} \left(\kappa \frac{\partial T}{\partial x} \right) = -f(T, j), \quad (3)$$

$$f(T, j) = -j^2(t) \rho(T) + d^{-1} q(T); \quad j(t) \langle \rho \rangle = U/L.$$

Here $j(t)$ is the sample current, which is independent of x because of the condition of local electrical neutrality, $C_v(T)$ is the heat capacity of the metal per unit volume, $\alpha(T)$ is the thermal emf coefficient, $\kappa(T)$ is the thermal conductivity, $\rho(T) = \sigma^{-1}(T)$, U is the applied voltage, and L is the length of the sample. Here and subsequently, the brackets $\langle \dots \rangle$ indicate an average over x along the whole sample. The function $f(T, j)$ is the heat dissipation per unit length in the sample.

In the contactless case we must supplement the system (3) with the periodicity condition $T(x + L, t) = T(x, t)$. However, if the sample is connected to an external circuit, the boundary condition is the continuity of the heat flux at both ends of the sample. We shall not write down the expression for this condition, since if L is sufficiently large, the thermal-electric domains have the same structure independently of the means of producing the electric field in the sample. On the other hand, in the case of comparatively short samples, the new, contactless experimental apparatus is of greater physical interest. We shall, therefore, limit the further discussion to an analysis of the contactless situation.

§2. THERMAL-ELECTRIC DOMAIN STRUCTURE AND DYNAMIC I-V CHARACTERISTIC

The system of equations of the problem always has the steady-state homogeneous solution

$$T(x, t) = T_0(U), \quad j(t) = j_0(U) = \sigma(T_0) U/L, \quad f(T_0, j_0) = 0. \quad (4)$$

The last equation in (4) is identical to the energy balance condition (1). If at the point $T = T_0(U)$ the derivative $f' \equiv \chi' / (\sigma d)$ (here and subsequently, a prime denotes differentiation with respect to T), then, as can be seen from (3), the uniform temperature and electric field distribution is stable (in the small) for any sample length L . However, when $\chi'(T_0(U)) < 0$, (where $T_A < T_0(U) < T_B$; see Fig. 1), the homogeneous solution (4) is stable only for L less than some critical length.

$$L_{cr}(T_0) = 2\pi (-\kappa \sigma d / \chi')^{1/2}_{T=T_0}. \quad (5)$$

For $L > L_{cr}(U)$ the uniform temperature distribution becomes unstable against fluctuations constituting an arbitrary sum of harmonics $A_n(t) \exp\{i2\pi n x/L\}$ ($n = \pm 1, \pm 2, \dots$) with $|n| < L/L_{cr}$. A fluctuation with $|n| > L/L_{cr}$ or $n = 0$ (uniform fluctuation) does not destroy the stability of solution (4).

In the range of parameters $L > L_{cr}(U)$ a "cyclical" thermal-electric domain, moving with constant velocity s , can be stable:

$$T(x, t) = v(x - st, j_d), \quad v(x) = v(x + L),$$

$$j_d(U) = (U/L) \langle \rho(v) \rangle^{-1}, \quad (6)$$

where $v(x)$ satisfies the equation of motion of a particle of variable mass $\kappa(v)$ acted on by a potential force $f(v, j)$ and a friction force proportional to dv/dx :

$$\frac{d}{dx} \left(\kappa(v) \frac{dv}{dx} \right) + \left(C_v(v) s - j_d v \frac{d\alpha}{dv} \right) \frac{dv}{dx} = f(v, j_d) \quad (7)$$

(here x is the "time" and v is the "coordinate" of the particle). Postponing the proof of thermal-electric domain instability to Sec. 3, we proceed to determine the domain velocity s and investigate the dynamic I-V characteristic $j_d(U)$ corresponding to the domain regime.

In Eq. (7) the role of the particle "energy" is assumed by the quantity

$$E(x) = \frac{1}{2} \kappa^2(v) (dv/dx)^2 + W(v, j_d), \quad (8)$$

where the "potential energy" is

$$W(T, j) = - \int_{T_A(T)}^T \kappa(T') f(T', j) dT' \quad (9)$$

(the form of $W(T)$ is shown in Fig. 1). The change of energy with "time" is governed by the action of the "friction force":

$$dE/dx = -\kappa(v) (C_v(v) s - j_d v (d\alpha/dv)) (dv/dx)^2. \quad (10)$$

The velocity s of a cyclic domain is found from the condition that the total change of energy $E(x)$ in a "period" L vanish:

$$s = j_d \left\langle \kappa(v) v \frac{d\alpha}{dv} \left(\frac{dv}{dx} \right)^2 \right\rangle / \left\langle \kappa(v) C_v(v) \left(\frac{dv}{dx} \right)^2 \right\rangle. \quad (11)$$

As can be seen from (11), the velocity of a thermal-electric domain is $s \sim j\alpha/C_v$, which is in agreement with the esti-

mates given in Ref. 2. For a given U , Eq. (7) determines one or more cyclic domains (6).

The ratio of the "friction" force in Eq. (7) to the "inertial" term for any value of L is a quantity of the order

$$\xi = j\alpha L_0 / \kappa \sim \alpha (\sigma T_D / \kappa)^{1/2} \lesssim k T_D / \varepsilon_F, \quad (12)$$

where L_0 is the characteristic value of L_{cr} and ε_F is the characteristic Fermi energy. From this it follows that the function $v(x)$ satisfies an "energy" conservation law

$$\frac{1}{2} \left(\kappa(v) \frac{dv}{dx} \right)^2 + W(v, j_d) = E = \text{const} > 0. \quad (13)$$

with an accuracy to small corrections $\sim k T_D / \varepsilon_F$. In this approximation the domain velocity s is given by the formula

$$s = j_d \int_{v_{min}}^{v_{max}} T \alpha'(T) [E - W(T, j_d)]^{1/2} dT / \int_{v_{min}}^{v_{max}} C_v(T) [E - W(T, j_d)]^{1/2} dT, \quad (14)$$

where the limits of integration v_{min} and v_{max} , the minimum and maximum temperatures of a cyclic domain, are the real roots of the equation $W(v, j_d) = E$.

The dependence of the voltage on the current $U = U_d(j)$ in the domain regime can, with the accuracy cited above, be found from the solution to the system of equations

$$\tilde{L}(E, j) = \sqrt{2} \int_{v_{min}(j)}^{v_{max}(j)} \kappa(T) [E - W(T, j)]^{-1/2} dT = L, \quad (15)$$

$$\tilde{U}(E, j) = \sqrt{2} \int_{v_{min}(j)}^{v_{max}(j)} \rho(T) \kappa(T) [E - W(T, j)]^{-1/2} dT = U, \quad (16)$$

where $\tilde{L}(E, j)$ is the "period of motion" of a nonlinear oscillator with energy E . The solutions of the system of equations (15) and (16), $E = E_d(U, L)$ and $j = j_d(U, L)$, are, respectively, the "energy" of a domain and the current in the domain regime.

To investigate the dynamic I-V characteristic we exa-

mine first the family of level curves $\tilde{L}(E, j) = \text{const}$ in the plane of the variables (E, j) . According to (13) this family lies within the "domain" region bounded by the curves of the potential-energy maxima (see Fig. 1) $E = W_{1,3}(j) \equiv W(T_{1,3}(j), j)$ and the straight line $E = W(T_2(j), j) \equiv 0$ (these lines are designated I, II, and III in Fig. 2a). For $W_{1,3} - E \rightarrow 0$, the period $\tilde{L}(E, j)$ goes logarithmically to infinity. The regions $0 < E \ll W_0 = \min W_{1,3}(j)$ correspond to domains of small amplitude that vanishes on the straight line $E = 0$. As $E \rightarrow 0$ the extremal temperatures v_{min} and v_{max} in (15) and (16) converge to $T_2(j)$ and the period $\tilde{L}(E, j)$ approaches the value $L_{cr}(j)$ that coincides with the critical length (5) at the point $T = T_2(j)$. In the general case the function $\tilde{L}(E, j)$ can have extrema within the domain region. Simple topological considerations show that among the constant-value level curves there are self-intersecting separatrices that divide the entire domain region into a number of subregions of two types: the "α-type" subregion contains level curves whose ends lie on the line $E = 0$ (so-called α lines) and the "β-type" subregion contains closed level curves (so called β lines). The α type of subregion always borders on the bounding curves $E = W_1(j)$ and $E = W_3(j)$ (lines I and III in Fig. 2a). Thus, in the general case the lines $\tilde{L}(E, j) = L$ consist of several isolated α and β branches. An example of the division of the domain region into α and β subregions is shown in Fig. 2a.

By means of the mapping $U = \tilde{U}(E, j)$ defined by (16), each branch of a contour line generates the corresponding branch of the dynamic I-V characteristic in the U - j plane. In this mapping, the ends of the α branches lie on the static I-V characteristic $j = j_0(U)$ corresponding to a uniform temperature distribution. The differential resistance dU_d/dj of the dynamic I-V characteristic is expressed directly in terms of the derivatives of the functions \tilde{U} and \tilde{L} (Eqs. (15) and (16)):

$$\rho_d = dU_d/dj = \{ \tilde{U}, \tilde{L} \} / \tilde{L}'_E, \quad \{ \tilde{U}, \tilde{L} \} = \tilde{U}'_j \tilde{L}'_E - \tilde{U}'_E \tilde{L}'_j; \quad (17)$$

where the symbols f'_E and f'_j here and below denote, respectively, partial derivatives with respect to "energy" and current. In formula (17) the "energy" E of a domain is defined by the relation $L = \tilde{L}(E, j)$.

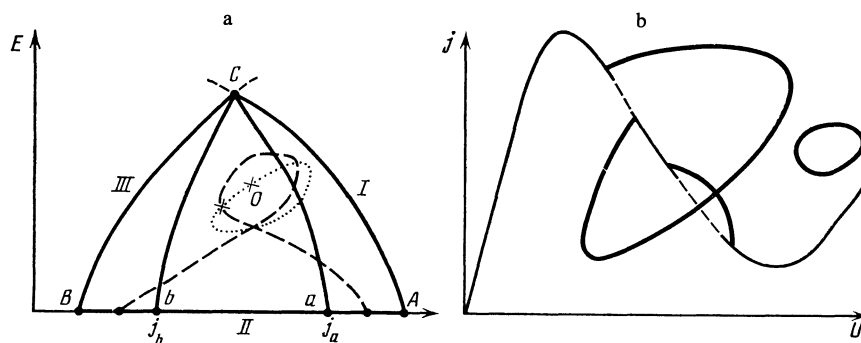


FIG. 2. a) Domain region in the plane of the parameters domain "energy" E and domain current j . Curves II and III are defined in the text. Curves Ca and Cb map out the lines with $dU_d/dj = 0$. The lines where $dU_d/dj = \infty$ are denoted by points. The contour line $\tilde{L}(E, j) = L$ having a self-intersection (separatrix) is indicated by the dashes. The point O is the extremal point of $\tilde{L}(E, j)$. The point C corresponds to the critical value j_{cr} of the current for which the potential maxima $W_1(j)$ and $W_3(j)$ coincide. The area within the curve Ca is the region of instability. b) Example of a dynamic I-V characteristic. The segments of instability of the uniform distribution are indicated by the dashed lines.

The positions of the α and β branches corresponding to a given value of L , relative to each other and to the static I-V characteristic, can be arbitrary. Moreover, the branches of the dynamic I-V characteristic can have self-intersections. For this to occur, there must exist special values of L and U for which $\tilde{L}'_E = \tilde{U}'_E = 0$ ($\tilde{L} = L, \tilde{U} = U$). At values of L corresponding to the separatrices of the domain region, the different branches of the dynamic I-V characteristic come together such that the points of juncture correspond to the points of self-intersection of the separatrix, where $\tilde{L}'_j = \tilde{L}'_E = 0$. According to (17), $\rho_d(j) = 0$ on the line $\{\tilde{L}, \tilde{U}\} = 0$. The extrema of the I-V characteristic correspond to the lines $\tilde{L}'_E = 0$. An example of a dynamic I-V characteristic having α and β branches is shown in Fig. 2b.

Let us consider in more detail the behavior of the dynamic I-V characteristic in the following limiting cases: a) small-amplitude domains, which are formed at

$$\eta = (L - L_{cr}(j)) / L \sim E / W_0 \ll 1;$$

b) domains which are formed in the limit when the characteristic critical length is $L_0 \ll L$.

In case a), to find the dynamic I-V characteristic we can expand in powers of $E \ll W_0$ in Eqs. (15)-(17) and consider only the first nonvanishing approximation. Because E is a positive quantity, small-amplitude domains exist only in the semi-infinite interval of current, where $(j_e - j)(\tilde{L}'_j, \tilde{L}'_E)|_{E=0, j=j_e} > 0$. The end point $j_e = j_e(L)$ of the interval is determined by the equality $L_{cr}(j_e) = L$, (where $L_{cr}(j_e) \equiv \tilde{L}(0, j_e)$). At this point $U_d(j_e) = U_0(j_e(L)) \equiv U_L$ (where $U_0(j)$ is the function that is the inverse of the static I-V characteristic) and $E_d(U, L) = 0$.

In the Appendix it is shown that the differential resistance (ρ_L) at the limit point j_e of the dynamic I-V characteristic vanishes for at least two values of L , $L = L_a$ and $L = L_b$. For values of L close to $L_{a,b}$ and of current close to $j_{a,b} = j_e(L_{a,b})$, the function $U_d(j)$ is parabolic. This means that there exists a small emf interval from U_L to $U_L + \Delta U$ (where $\Delta U \propto (L - L_{a,b})^2$) in which two small-amplitude domains, of energy E_d^+ and E_d^- differing by $\sim L - L_{a,b}$ correspond to each value of U .

Let us turn now to case b) ($L \gg L_0$). Since the period $\tilde{L}(E, j)$ of the nonlinear oscillator (see (15)) diverges logarithmically as $E \rightarrow \min W_{1,3}(j)$ (where $W_{1,3}$ are the maxima of the "potential" energy $W(T, j)$), in the limit $L \gg L_0$ the "energy" $E = E(L, j)$ of a domain must differ from $\min\{W_1, W_3\}$ by an exponentially small amount. If the current j is not too close to the critical current j_c for which $W_1(j_c) = W_3(j_c)$, then, with accuracy exponential in the parameter $L/L_0 \gg 1$, the thermal-electric domain is described by the soliton solution, $v_{sol}(x)$ of Eq. (13), corresponding to the "energy" $E = \min(W_1(j), W_3(j))$. As $x \rightarrow \pm \infty$ the function v_{sol} coincides with the temperature of the least of the maxima; it differs substantially from a constant value in the region $\sim L_0$. The dynamic I-V characteristic corresponding to this soliton coincides, to within $\sim L_0/L \ll 1$, with one of the rising segments of the static I-V characteristic (for $j_c < j < j_A$ with the left segment, and for $j_B < j < j_c$ with the right segment; see Fig. 3). The transition between the segments takes place

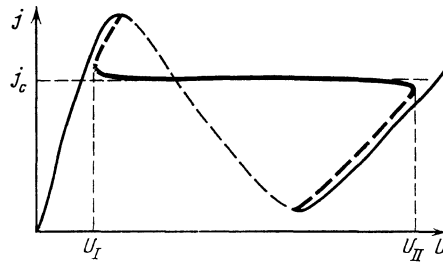


FIG. 3. I-V characteristic for $L \gg L_0$. The dashes indicate the regions of instability of the dynamic and static I-V characteristics. The light solid lines are the stable segments of the static I-V characteristic and the heavy solid lines are the stable segments of the dynamic I-V characteristic. The quantity j_c is the critical current corresponding to the point c of Fig. 2a.

in a very narrow current interval that contains the point j_c (see Fig. 3). It is not difficult to obtain from (15) and (16) the equation for the behavior of the dynamic I-V characteristic over the entire region $|j - j_c| \ll j_c$ if one takes into account that the temperatures v_{min} and v_{max} are close to the maxima of the "potential" $W(T)$, i.e., T_1 and T_3 , respectively. After a simple calculation we obtain

$$j - j_c = J_I \exp \left\{ -\frac{\lambda_1 (U - j \rho_1 L)}{j_c (\rho_3 - \rho_1)} \right\} - J_{II} \exp \left\{ \frac{\lambda_3 (U - j \rho_3 L)}{j_c (\rho_3 - \rho_1)} \right\}, \quad (18)$$

where $\rho_{1,3} = \rho(T_{1,3})$, $\lambda_{1,3} = f'(T_{1,3}, j_c)$ and the constants $J_{I,II}$ are $\sim j_c$. Equation (18) gives the dynamic I-V characteristic in implicit form. It can be seen from (18) that for all values U of the emf in the interval $U_I < U < U_{II}$ (where $U_I = j_c \rho_1 L$ and $U_{II} = j_c \rho_3 L$), except for a small region near the ends of the interval, the current j coincides with j_c to an accuracy exponential in the parameter L/L_0 . Near the points U_I and U_{II} there is a sharp transition from the nearly horizontal segment of the dynamic I-V characteristic to the rising segments mentioned above (see Fig. 3). The values of current

$$j = j_I = j_c [1 + (\rho_3 - \rho_1) / \rho_1 \lambda_1 L], \quad j = j_{II} = j_c [1 + (\rho_1 - \rho_3) / \rho_3 \lambda_3 L], \quad (19)$$

which differ from the critical current by the amount $\sim j_c (L_0/L)$, correspond to the points of the I-V characteristic having a vertical tangent.

The fact, mentioned above, that the current is independent of the emf in the interval $[U_I, U_{II}]$, comes about because in this region the domain structure undergoes a substantial modification. The point is that in the limit as $L \rightarrow \infty$ and at $j = j_c$ Eq. (13) with "energy" $E = W_1(j_c) = W_3(j_c)$ has two domain-wall type solutions:

$$\theta_c^+ = \theta_c(x - x_+), \quad \theta_c^- = -\theta(x - x_-) + T_{1c} + T_{3c}, \quad (20)$$

$$\lim_{x \rightarrow +\infty} \theta_c(x) = T_{1c} = T_1(j_c), \quad \lim_{x \rightarrow -\infty} \theta_c(x) = T_{3c} = T_3(j_c),$$

where the parameters x_{\pm} are arbitrary ($x_- < x_+$) and the function $\theta_c(x)$ varies from T_1 to T_3 in an interval $\sim L$. For a current close to j_c a thermal-electric domain appears as two coupled domain walls v_- and v_+ ; it has a trapezoidal shape and consists of two planar segments with temperatures that differ from $T_1(j)$ and $T_3(j)$ by an amount $\sim |j - j_c|$. In the narrow transition regions of width $\sim L_0$ the thermal-electric

domain coincides, to the same accuracy, with $\theta_c^+(x - x_+)$ and $\theta_c^-(x - x_-)$. For this reason a variation of the emf causes a change mainly only in the lengths of the planar segments, $L_I = x_+ - x_-$ and $L_{II} = L - (x_+ - x_-)$, of the trapezoidal domain. The dependence of L_I and L_{II} on U can be easily found directly from (6) by neglecting the contribution of the transition region in the total potential drop in the sample:

$$L_I = (U - U_I)/j_c(\rho_s - \rho_i), \quad L_{II} = (U - U_{II})/j_c(\rho_i - \rho_s). \quad (21)$$

In this approximation these formulas are applicable in the entire range of U where $L_{I,II} \geq 0$, i.e., in the interval $[U_I, U_{II}]$. The velocity s of a trapezoidal domain is, with accuracy exponential in L_0/L , independent of the length of the planar segments and can be expressed directly in terms of the characteristics of the sample (in formula (14) one should set $j = j_c$ and $W = W_c \equiv W_1(j_c) = W_3(j_c)$).

To conclude this section we shall estimate the basic parameters of a thermal-electric domain. When L is of the order of the spatial scale L_0 , the characteristic temperature of a domain, as follows from the form of $\chi(T)$ (see Sec. 1), is of the order of the Debye temperature, the length is

$$L_0 \sim (2\pi)^2 d T_D \kappa(T_D) / q(T_D), \\ s \sim \alpha(T_D) [q(T_D) \sigma(T_D)]^{1/2} C_v^{-1}(T_D) d^{-1/2}, \quad (22)$$

and the time for the instability to develop is

$$\tau \sim d T_D C_v(T_D) / q(T_D).$$

From this it can be seen that as the characteristic thickness d of the sample decreases the spatial and time scales L_0 and τ decrease in proportion to d , while the domain velocity s increases as $d^{-1/2}$. For a heat outflow $q(T_D) \sim 1 \text{ W/cm}^2$ and $d \sim 10^{-2} \text{ cm}$ we have $\tau \sim 1 \text{ sec}$, $L_0 \sim 1 \text{ cm}$ and $s \sim 10^{-1}$ to 10^{-2} cm/sec . The estimate for the velocity s agrees with the experimental data of Ref. 6.

In the limit $L \gg L_0$, according to the above discussion, the thermal electric domain consists of two planar segments with sharply differing temperatures, $T_1 \sim T_A \approx 4.2 \text{ K}$ and $T_3 \sim T_B \sim T_D \gg T_A$ (see Fig. 1). However, the main contribution to the velocity s , as is seen from formula (14), is made by the high-temperature region. Since the critical current is $j_c \sim j_B$, the estimate for s given above is also valid in this case.

As follows from the preceding estimates, the velocity of a thermal-electric domain increases with the thermal emf coefficient α . In this respect principal interest attaches to quasi-one-dimensional metal conductors⁸ having a thermal emf that is three orders of magnitude greater than ordinary metals with low anisotropies. Another interesting aspect of thermal-electric instabilities in quasi-one-dimensional conductors is the low sensitivity of the moving thermal-electric domains to the thickness of the sample. This latter feature is due to the fact that in a quasi-one-dimensional conductor the direction of the current is fixed with high precision.

It is interesting to note that because the thermal conductivity transverse to a quasi-one-dimensional conductor filaments is relatively low, the transverse dimensions of the region that governs the development of the thermal-electric instability turns out to be substantially less than the thickness of the sample.

In the presence of a strong magnetic field such that $\Omega_H t_{im} \gg 1$ (where Ω_H is the cyclotron frequency), the I-V characteristics of metals of conductivity $\sigma \sim \sigma_0 / (\Omega_H \bar{t})^2$ has, at $T = T(\mathcal{E}) \sim T_A$, an S-shaped segment (here $\bar{t}^{-1} \sim t_{im}^{-1} + t_{ep}^{-1}(T)$) and σ_0 is the conductivity at $H = 0$). On this segment the thermal-electric instability leads not to the formation of thermal-electric domains, but to a pinching of the current across the sample.

§3. THERMAL-ELECTRIC DOMAIN STABILITY

To investigate the stability of thermal-electric domains, we introduce the dimensionless variable $\varphi = 2\pi x/L$ and write Eq. (3) in the form

$$C_v \frac{\partial T}{\partial t} + \frac{2\pi j(t) T \alpha'}{L} \frac{\partial T}{\partial \varphi} - \left(\frac{2\pi}{L} \right)^2 \frac{\partial}{\partial \varphi} \left(\kappa(T) \frac{\partial T}{\partial \varphi} \right) = -f(T, j), \quad (23)$$

$$j(t) \langle \rho(T) \rangle_\varphi = U/L, \quad (24)$$

where $T(\varphi, t) = T(\varphi + 2\pi, t)$. The operation $\langle \dots \rangle_\varphi$ denotes an average over φ (henceforth we shall omit the subscript φ on the angle brackets).

We represent the temperature distribution in the sample in the form of a sum

$$T(\varphi, t) = \theta(\varphi) + \kappa^{-1}(\theta(\varphi)) \theta_1(\varphi, t), \quad (25)$$

where $\theta(\varphi) \equiv \vartheta(L\varphi/2\pi)$ is a thermal-electric domain (6) and $\kappa^{-1}\theta_1$ is a small correction. After substituting (25) in (23) we obtain the following linearized equation for θ_1 :

$$\partial \theta_1 / \partial t + \beta(\varphi) \hat{H} \theta_1 = 2\bar{j} \rho(\theta) \beta(\varphi) j_1(t). \quad (26)$$

Here the Hermitian operator is

$$\hat{H} = \left(\frac{2\pi}{L(\bar{E}, \bar{j})} \right)^2 \frac{\partial^2}{\partial \varphi^2} + V(\varphi), \quad V(\varphi) \equiv \frac{f'(\theta(\varphi), \bar{j})}{\kappa(\theta(\varphi))}, \\ \beta(\varphi) = \kappa(\theta(\varphi)) / C_v(\theta(\varphi)) > 0, \quad (27)$$

and j_1 is a small, time-dependent increment to the current:

$$j_1(t) = -\bar{j} \left\langle \frac{\rho'(\theta)}{\kappa(\theta)} \theta_1 \right\rangle / \langle \rho(\theta) \rangle. \quad (28)$$

In writing down the linearized equation (26) we have introduced as the independent parameters the "energy" \bar{E} of a domain and the current \bar{j} in the domain regime (see (15) and (16)) instead of the sample length L and the emf U . In addition, we have dropped the small term proportional to ξ (see (12)), which only weakly changes the positions of the stability boundaries of the thermal-electric domains in the space of the parameters of the problem. With the same degree of accuracy we can assume that the function $\theta(\varphi) = \theta(\varphi + 2\pi)$ that enters into (26)–(28) is governed by the reduced time-independent equation

$$\left(\frac{2\pi}{L(\bar{E}, \bar{j})} \right)^2 \frac{d}{d\varphi} \left(\kappa(\varphi) \frac{d\theta}{d\varphi} \right) = f(\theta, \bar{j}), \quad (29)$$

which, when integrated with account taken of the 2π -periodicity of $\theta(\varphi)$, leads to a conservation law with the "energy" \bar{E} equal to

$$\frac{1}{2} \left(\frac{2\pi}{\mathcal{L}(\bar{E}, \bar{j})} \right)^2 \left(\kappa \frac{d\theta}{d\varphi} \right)^2 + W(\theta, \bar{j}) = \bar{E}. \quad (30)$$

Let us write $\theta_1(\varphi, t)$ in the form of an expansion

$$\theta_1(\varphi, t) = \sum_{\nu} a_{\nu}(t) \psi_{\nu}(\varphi), \quad (31)$$

where ψ_{ν} are the eigenfunctions of the operator $\hat{H}_{\beta} = \beta(\varphi) \hat{H}$, which satisfies the Sturm-Liouville equation

$$\left[\left(\frac{2\pi}{\mathcal{L}(\bar{E}, \bar{j})} \right)^2 \frac{d^2}{d\varphi^2} + V(\varphi) \right] \psi_{\nu} = \lambda_{\nu} \beta^{-1} \psi_{\nu} \quad (\beta > 0). \quad (32)$$

The subscript $\nu = 0, 1, 2, \dots$ enumerates the eigenvalues λ_{ν} in ascending order. Substituting (31) into (26) and carrying out a Laplace transformation with respect to t , and then after carrying out a series of calculations taking into account that the Hermitian conjugate operator $\hat{H}^{\dagger} = \hat{H}\beta(\varphi)$ has the eigenfunctions $\bar{\psi}_{\nu} = \beta^{-1} \psi_{\nu}$, we find

$$j_1(p) = - \frac{\bar{j}}{\langle \rho(\theta) \rangle} \sum_{\nu} \frac{a_{\nu}(0) \langle \rho'(\theta) \kappa^{-1}(\theta) \psi_{\nu} \rangle}{p + \lambda_{\nu}} \times \left(1 + \sum_{\nu} \frac{A_{\nu}}{p + \lambda_{\nu}} \right)^{-1}, \quad (33)$$

where $j_1(p)$ is the Laplace transform of the function $j_1(t)$,

$$A_{\nu} = 2\bar{j}^2 \langle \psi_{\nu} \kappa^{-1}(\theta) \rho'(\theta) \rangle / \langle \rho(\theta) \rangle \mathcal{L}, \quad (34)$$

and $a_{\nu}(0)$ is the initial value of $a_{\nu}(t)$. It can be seen from expression (33) that for stability of the domain distribution in the small it is necessary and sufficient that the function

$$Q(p) = 1 + \sum_{\nu} A_{\nu} (p + \lambda_{\nu})^{-1} \quad (35)$$

have no zeros in the half-plane $\text{Re } p > 0$.

To analyze the behavior of $Q(p)$ we use a well known theorem on the number of zeros of the eigenfunctions of the Sturm-Liouville operator with periodic boundary conditions.⁹ According to this theorem, $\psi_0(\varphi)$ (the ground state) has no zeros while the remaining $\psi_{\nu}(\varphi)$ are grouped in pairs: for $\nu = (2k - 1)$ and $2k$ the number of zeros of $\psi_{\nu}(\varphi)$ is $2k$. On the other hand, from the translational symmetry of the time-independent equation (29) it follows that the eigenfunctions of the operator \hat{H}_{β} include the function

$$\Phi(\varphi) = \kappa(\theta(\varphi)) \partial\theta/\partial\varphi, \quad (36)$$

corresponding to the eigenvalue $\lambda_{\nu} = 0$. Since $\theta(\varphi)$ has only two extrema, the minimal eigenvalue λ_0 is necessarily negative while the eigenvalue $\lambda_{\nu} = 0$ has the index $\nu = 1$ or 2 . All the constants A_{ν} (see (34)) as well as the eigenfunctions $\psi_{\nu}(\varphi)$ are real, with $A_0 = 0$ corresponding to the ground state ψ_0 , which has no zeros, while $A_{\nu} = 0$ corresponds to the function $\psi_{\nu} = \Phi(\varphi)$ ($\nu = 1$ or 2). The last equality means that the function $Q(p)$ has at $\text{Re } p > 0$ only one (two) singularities at the points $p = -\lambda_0$ ($p = -\lambda_1$ for $\lambda_2 = 0$). It is also essential that A_0 be positive, because in the contrary case the function $Q(p)$ would have a zero at some point $p > -\lambda_0$ and the thermal-electric domain would be unstable. The rest of the A_{ν} in the general case are arbitrary within the limits of the inequality

$$\sum_{\nu} A_{\nu} = \frac{2\bar{j}^2 \langle \rho(\theta) \rho'(\theta) C_{\nu}^{-1}(\theta) \rangle}{2\pi \mathcal{L} \langle \rho(\theta) \rangle} > 0,$$

which follows from the fact that ρ, ρ' , and C_{ν} are positive.

It is possible to draw some general conclusions concerning the location of the regions of stability of thermal-electric domains in the plane of the parameters (\bar{E}, \bar{j}) if we note that the number of zeros of the function $Q(p)$ in the half-plane $\text{Re } p > 0$ changes by unity if the quantity

$$Q(0) = \frac{dU_d(\bar{j})}{d\bar{j}} \frac{1}{\langle \rho \rangle} \quad (37)$$

(formula (37) is derived in the Appendix) changes sign, while the number of singularities of $Q(p)$ (for $\text{Re } p > 0$) remains unchanged. According to (37) and (17), $Q(0)$ is reflected at 0 and ∞ , respectively, in the lines

$$\{U(\bar{E}, \bar{j}), \mathcal{L}(\bar{E}, \bar{j})\} = 0 \quad (dU_d/dj = 0) \quad (38)$$

and

$$\mathcal{L}'(\bar{E}, \bar{j}) = 0 \quad (dU_d/dj = \infty). \quad (39)$$

The number of zeros of $Q(p)$ for $\text{Re } p > 0$ changes, however, only upon crossing the line (38). Actually, differentiating Eq. (29) with respect to \bar{E} and keeping in mind the definition of the operator \hat{H} (27), we see that at $\mathcal{L}'(\bar{E}, \bar{j}) = 0$, not only the function $\Phi(\varphi)$ but also the function $\psi(\varphi) = \kappa(\theta) (\partial\theta/\partial\bar{E})|_{\bar{j}}$ corresponds to the eigenvalue $\lambda_{\nu} = 0$. Upon displacement from the line (39), the twofold degeneracy of the level $\lambda_{\nu} = 0$ is lifted and the number of positive singular points of $Q(p)$ (i.e., negative λ_{ν}) increases (decreases) by one. In the general case this does not change the number of zeros of $Q(p)$ in the region $\text{Re } p > 0$ and does not affect the stability of the thermal-electric domain.

Thus, we arrive at the conclusion that the region of unstable thermal-electric domains is adjacent to the line (38) in the plane of the parameters (\bar{E}, \bar{j}) on at least one side. Consequently, at least one of the dynamic I-V characteristic branches which come together at the point with the vertical tangent must be unstable. The extremal points of the dynamic I-V characteristic, however, as regards thermal-electric domain instability are not distinguished in any way.

Equation (38), generally speaking, defines several isolated curves in the (\bar{E}, \bar{j}) plane. In particular, as follows from the analysis presented in Sec. 2, two lines (38) must terminate at the point $\bar{E} = W_1(j_c) = W_3(j_c), \bar{j} = j_c$. In addition, according to the discussion of small-amplitude domains in Sec. 2, two lines (38) must terminate on the straight line $\bar{E} = 0$ at the points $(0, j_a)$ and $(0, j_b)$. An example of a possible arrangement of the regions of stability of thermal-electric domains is shown in Fig. 2.

Of course, the number of zeros of the function $Q(p)$ in the half-plane $\text{Re } p > 0$ can change not only when the function $Q(0)$ vanishes. For example, in the case $\lambda_1 < 0$ the zeros of $Q(p)$ (for $\text{Re } p > 0$) appear (or disappear) also when the coefficient A_1 changes sign. In the general case the positions of the stable and unstable segments of the dynamic I-V characteristic are quite arbitrary. In particular, it can happen that for a given U there are only unstable segments of the

static and dynamic I-V characteristics. In this case, clearly, a non-steady-state turbulent situation arises in the system.

In the limit $L \gg L_0$, as follows from the analysis given in Sec. 2, the operator $V(\varphi)$ (see (27)) corresponding to a thermal-electric domain of the soliton form (i.e., to the branches of the dynamic I-V characteristic near the static characteristic, Fig. 3) is a system of periodically repeated potential wells of width $\sim L_0$ spaced a distance $\sim L$ apart. Here the eigenvalues λ_ν coincide approximately with the eigenvalues of the operator $\hat{H}_\beta = \beta(\varphi)\hat{H}$, which is obtained by replacing $V(\varphi)$ with the potential of one of the wells. Consequently, all the λ_ν , except λ_0 are non-negative, and now the necessary condition for stability of a thermal-electric domain is that Q_0 be negative. As can be seen from (37), the condition is not satisfied in this case, i.e., thermal-electric domains of the soliton type are unstable.

In the case of trapezoidal thermal-electric domains corresponding to the interval $[U_I, U_{II}]$ (see Fig. 3) the potential $V(\varphi)$ over the range of a single period has the following form: In the intervals $[\varphi_-, \varphi_+]$ and $[\varphi_+, \varphi_- + 2\pi]$, (where $\varphi_\pm = 2\pi x_\pm / L$, see Sec. 2), except for a small neighborhood of their ends, the potential $V(\varphi)$ is, respectively,

$$V_3 = f'(T_{3c}, j_c) / \kappa(T_{3c}) > 0 \quad \text{and} \quad V_1 = f'(T_{1c}, j_c) / \kappa(T_{1c}) > 0.$$

According to the discussion of Sec. 2, the temperature $T_{3c} \sim T_D$ is much higher than the temperature $T_{1c} \sim T_A$, and the ratio is

$$\frac{V_1}{V_3} \sim \frac{T_D}{T_A} \sigma(T_D) \kappa(T_D) / \sigma(T_A) \kappa(T_A) \ll 1.$$

In the transition regions $V(\varphi)$ is a set of potential wells with characteristic width

$$\Delta\varphi \sim 2\pi L_0 / L \ll (\varphi_+ - \varphi_-), \quad (2\pi + \varphi_- - \varphi_+)$$

and depth $\sim V_3 \gg V_1$. Here the potential wells near the points φ_- and φ_+ are symmetric relative to $(\varphi_- + \varphi_+) / 2$. From this it follows that the structure of the spectrum of λ_ν and of the eigenfunctions ψ_ν is the following: the minimal eigenvalue $\lambda_0 < 0$ lies exponentially (in the parameter $L_0/L \ll 1$) close to $\lambda_1 = 0$, the eigenfunctions ψ_0 and ψ_1 are different from zero only in the transition regions noted above and, up to corrections that are exponentially small in the parameter L_0/L , are of the form

$$\psi_0 = \frac{\partial \bar{\theta}_c^-}{\partial \varphi} - \frac{\partial \bar{\theta}_c^+}{\partial \varphi}, \quad \psi_1 = \frac{\partial \theta}{\partial \varphi} \approx \frac{\partial \bar{\theta}_c^+}{\partial \varphi} + \frac{\partial \bar{\theta}_c^-}{\partial \varphi},$$

$$\bar{\theta}_c^\pm \equiv \theta_c^\pm \left(\frac{L\varphi}{2\pi} \right),$$

where $\theta_c^\pm(x)$ is domain-wall type of solution [Eqs. (20) and (21)]. All the rest of the eigenfunctions ψ_ν whose coefficients A_ν (see (34)) are not small differ from zero in the interval $[\varphi_+, \varphi_- + 2\pi]$, where the temperature $\theta(\varphi) \approx T_{1c}$. The corresponding A_ν are positive. Summing the A_ν and taking it into account that $Q(0) = -A_0/|\lambda_0|$, it is not difficult to conclude that $Q(p)$ does not vanish in the half-plane $\text{Re } p > 0$. Consequently, trapezoidal domains are stable in the small.

The stability of small-amplitude domains is investigated in Sec. 4 within the framework of a general theory which

describes the dynamics of their development.

The entire discussion above has pertained to thermal-electric domains which correspond to a single revolution of a "particle" in a closed trajectory (13) in the phase plane $\theta, \partial\theta/\partial x$, i.e., the "period" $\tilde{L}(E, j) = L$. In the case $\tilde{L}(E, j) = L/n$ (where $n = 2, 3, \dots$), "multiple" thermal-electric domains, obtained by an n -fold repetition of the function $\theta(x)$ (with period \tilde{L}), are also possible in principle. An analysis similar to that above shows that for all the multiple thermal-electric domains, the function $Q(p)$ is identical with the $Q(p)$ that corresponds to the case $\tilde{L} = L$. However, they are unstable for arbitrarily small sample nonuniformities and are therefore of no interest to us.

§4. EVOLUTION OF SMALL-AMPLITUDE THERMAL-ELECTRIC DOMAINS

In the case of small-amplitude thermal-electric domains (see Sec. 2) it proves possible not only to find criteria for stability of the thermal-electric domains in the small, but also to study the evolution of the thermal-electric domains for any initial conditions in which the characteristic temperature variation is comparable to the domain amplitude. The smallness of the parameter η (see Sec. 2) permits an abbreviated description of domain instability; the essence of this description is the following.

We represent the temperature distribution in the sample as a sum $T(\varphi, t) = T_2 j(t) + \tilde{T}(\varphi, t)$, where φ is the dimensionless variable introduced in Sec. 3, and the increment $\tilde{T}(\varphi, t) \ll T_2$. Expanding $\tilde{T}(\varphi, t)$ in a Fourier series

$$T(\varphi, t) = \sum_{n=-\infty}^{+\infty} A_n(t) \exp\{in(\varphi - \Omega t)\}, \quad (40)$$

where the frequency $\Omega = s/L$ and s is the domain velocity, see (14), and substituting $T = T_2 + \tilde{T}$ in Eqs. (23) and (24), we obtain for the amplitudes of the harmonics a system of nonlinear differential equations of the form

$$dA_n/dt = t_n^{-1} A_n + \sum_{r=2}^{\infty} \sum_{i_1+\dots+i_r=n} F_r A_{i_1} A_{i_2} \dots A_{i_r} \quad (n \neq 0), \quad (41)$$

$$dA_0/dt = t_0^{-1} A_0 + \sum_{r=2}^{\infty} \sum_{i_1+\dots+i_r=0} K_r A_{i_1} A_{i_2} \dots A_{i_r},$$

where the summation is over all the indices i_1, \dots, i_r that satisfy the condition $i_1 + i_2 + \dots + i_r = n$, and the quantities t_0 and t_n are defined, accurate to $\sim \eta \xi \ll 1$ (where ξ is the parameter in (12)), by the equations

$$\frac{1}{t_0} = - \frac{\sigma q' - \sigma' q}{d\sigma C_v} < 0,$$

$$\frac{1}{t_n} = (2\pi)^2 \frac{\kappa}{C_v} \left[\frac{1}{L_{cr}^2(j(t))} - \frac{n^2}{L^2} \right], \quad n \neq 0. \quad (42)$$

All the functions of temperature in (41) and (42) are taken at the point $T = T_2(j(t))$. The coefficients are $F_r \sim K_r \sim 1/(T_2^{-1} t_0)$; their specific form is not essential for the subsequent discussion. All the t_n with $n \neq \pm 1$ (including $n = 0$) are negative and have a characteristic value $\sim \tau_0 = (C_v /$

κL_0^2 , the characteristic time of instability development. In contrast, t_1 is positive and large relative to the parameter η namely, $t_1 \sim \tau_0/\eta \gg t_0$. For this reason, the evolution of the Fourier coefficients $A_n(t)$ is governed by two processes, a slow variation of the amplitudes $A_{\pm 1}$, which takes place over a time $\sim t_1$, and a fast (in a time $\sim \tau_0$) adjustment of the rest of the amplitudes towards the instantaneous values of $A_{\pm 1}$. Thus for $t \gg \tau_0$ all the functions $A_n(t)$ with $n \neq \pm 1$ "forget" their original values and are expressed algebraically in terms of $A_1(t)$ and $A_2(t)$. The functions $A_{\pm 1}(t)$ themselves satisfy a system of two nonlinear first order differential equations. It is not necessary to write down this system of equations, since the slow change of $A_{\pm 1}(t)$ with respect to the parameter $\eta \ll 1$ and the smallness of the parameter $\xi \sim \Omega \tau_0$ mean that to find the solution of the system (23) and (24) for $t \gg \tau_0$ we can develop an adiabatic perturbation theory, writing

$$T(\varphi, t) = \theta(\varphi - \lambda(t), E(t), j(t)) + \theta_1(\varphi, t). \quad (43)$$

Here θ is a 2π -periodic function of φ that satisfies the equation obtained from (29) by the substitution

$$\bar{E} \rightarrow E(t), \quad \bar{j} \rightarrow j(t), \quad (44)$$

and the "energy" $E(t)$ is a slowly varying function of time and is to be determined along with the phase shift $\lambda(t)$ (the rate of change of the latter is $\propto \xi \ll 1$). The quantity $\theta_1(\varphi, t)$ is a correction that is small in the parameters ξ and η . According to the definition of θ and formula (24) the current $j(t)$ in the first approximation in η and ξ is related to $E(t)$ by the relation

$$\bar{U}(E(t), j(t)) / \bar{L}(E(t), j(t)) = U/L, \quad (45)$$

where \bar{L} and \bar{U} are functions defined by Eqs. (15) and (16).

The equations for $E(t)$ and $\lambda(t)$ are obtained from the requirement that the ratio $\theta_1 / \max|\theta - T_2|$ be small. Writing $\theta_1 = \kappa^{-1}(\theta) \Delta(\varphi, t)$ and substituting (43) in (23) we find in the first approximation in η and ξ

$$\begin{aligned} \hat{H}\Delta = & -C_v(\theta) \frac{\partial \theta}{\partial E} \frac{\partial E}{\partial t} - C_v(\theta) \frac{\partial \theta}{\partial j} \frac{\partial j}{\partial t} \\ + & \left[\left(\frac{2\pi}{L} \right)^2 - \left(\frac{2\pi}{\bar{L}} \right)^2 \right] \frac{\partial}{\partial \varphi} \left(\kappa(\theta) \frac{\partial \theta}{\partial \varphi} \right) \\ & + \left(C_v(\theta) \frac{d\lambda}{dt} - \frac{2\pi j T \alpha'}{L} \right) \frac{\partial \theta}{\partial \varphi}, \quad (46) \end{aligned}$$

where \hat{H} is an operator that differs from the operator of (27) by the replacement $\bar{L}(\bar{E}, \bar{j}) \rightarrow \bar{L}(E(t), j(t))$. As follows from the discussion in Sec. 3, the equation $\hat{H}\Delta = 0$ has a nontrivial solution $\Phi(\varphi) = \kappa(\theta) (\partial \theta / \partial \varphi)_{E, j}$. On the other hand, differentiating Eq. (29) with respect to the "energy", we have

$$\hat{H}\psi = \frac{8\pi^2}{\bar{L}^3} \left(\frac{\partial \bar{L}}{\partial E} \right)_j \frac{\partial}{\partial \varphi} \left(\kappa(\theta) \frac{\partial \theta}{\partial \varphi} \right), \quad \psi = \kappa(\theta) (\partial \theta / \partial E)_{\varphi, j}. \quad (47)$$

In the case we are studying, where the energy E is small, the right-hand expression of (47) is proportional to \sqrt{E} , as can be seen from (30). However, the value of the function ψ is proportional to $1/\sqrt{E}$, as follows directly from the differentiation of Eq. (30) with respect to E . Therefore, as can be seen from (46), the correction to θ is small in comparison with θ if

the right hand part of (46) is orthogonal not only to the function Φ but also to ψ . After some simple calculations, carried out in the first approximation in η and taking (45) into account, these two conditions lead to the equations

$$dE/dt = E(L - \Lambda(E)) / \tau L, \quad \Lambda(E) \equiv \bar{L}(E, j(E)); \quad (48)$$

$$d\lambda/dt = \Omega(t), \quad \Omega(t) = s(t)/L. \quad (49)$$

The function $j(E) = j(E; U, L)$ is defined implicitly by Eq. (45), and the velocity $s(t) = s(E(t), j(t))$, where $s(E, j)$ is the function (14). The constant

$$\tau = C_v(T_0) L_{cr}^2(j_0) / (16\pi^2 \kappa(T_0)) \sim \tau_0,$$

where $j_0 = j_0(U, L)$, $T_0 = T_0(U, L)$ are, respectively, the current and the temperature of the uniform distribution for given values of U and L .

Equation (48) is easy to reduce to quadratures:

$$t = \tau L \int_{E_0}^E \frac{dE'}{E'(L - \Lambda(E'))}, \quad (50)$$

where E_0 is the value of $E(t)$ at $t = 0$. Equation (48) is applicable in the entire "energy" region $0 \leq E \leq W_0$. It always has a stationary point $E = 0$ corresponding to a uniform temperature distribution. The other stationary point of $\bar{E}(L, U)$, the zero of the function $L - \Lambda(E)$, is the "energy" of the thermal-electric domain. Because Eq. (45) goes over to the equation $U(E, j) = U$ at $\Lambda(E) = L$, the region of parameters in which this second (nontrivial) zero occurs has already, in essence, been studied in Sec. 2 with the domain "energy" and domain current as variables. According to (48) the uniform state is stable at $L < \Lambda(0) \equiv L_{cr}(j_0(U, L))$, which, of course, agrees with the results of Sec. 2. A small-amplitude domain is stable if

$$\left(\frac{d\Lambda}{dE} \right) \Big|_{E=\bar{E}} = \{ \bar{U}, \bar{L} \} \left(\frac{\partial U_0}{\partial j} \right)^{-1} > 0, \quad (51)$$

where $\{ \bar{U}, \bar{L} \}$ are the Poisson brackets of (17) for values of E and j that satisfy Eqs. (15) and (16). In this case, any initial distribution, including those arbitrarily close to a uniform distribution, will evolve as $t \rightarrow \infty$ to a thermal-electric domain with $E = \bar{E}(U, L)$. From this discussion it follows that the line (38) in the region of small E is the boundary of the thermal-electric domain stability region. If the inequality opposite to (51) is satisfied, then the domain is unstable and the uniform state ($E = 0$) is stable. In this case, all distributions that occur in the limits $t_1 \gg t \gg \tau_0$, after shortening the description, are divided into two classes. The states with $E_0 < \bar{E}$ (where $E_0 > 0$) are transformed in the limit as $t \rightarrow \infty$ into the uniform distribution. The "energies" of the states with $E_0 > \bar{E}$ increase as an explosive instability: $E(t, E_0)$ goes to infinity in a finite time

$$t_0(E_0) = [\tau L / |L - L_{cr}(U)|] \ln [E_0 / (E_0 - \bar{E})] \sim t_1.$$

In this case at $t \sim t_0(E_0)$ a large-amplitude thermal-electric domain develops in the system or the system goes over into the turbulent regime (see Sec. 3).

According to the results of Sec. 2, for sample lengths L that are close to the selected values L_a or L_b and for domain currents $j \approx j_{a,b}$ there can exist a narrow range of U in which

each value of U corresponds to two small-amplitude domains. From Eq. (48) it follows directly that one of these domains is necessarily stable and the other unstable. If the uniform state is stable the domain with the smallest "energy" is unstable. When the uniform state is unstable this domain is stable. In the first case all the states of the system with initial "energy" $E_0 < E_{\min} = \min(E^+, E^-)$ approach asymptotically the uniform state, while the states with $E_0 > E_{\min}$ approach asymptotically the state of "energy" $E_{\max} = \max(E^+, E^-)$. In the second case all the states with E_0 in the band $0 < E < E_{\max}$ are transformed into a domain with "energy" $E = E_{\min}$, and the energies of the states with $E_0 > E_{\max}$ increase explosively as in the situation examined above for a single (unstable) domain.

In conclusion let us discuss briefly the dynamics of thermal-electric domains that occur in the presence of nonuniformities in the sample. It is physically obvious that the effect of a nonuniformity on the dynamics of a thermal-electric domain is determined by the relation between the velocity of a thermal-electric domain and the magnitude of the nonuniformity. As has already been mentioned, the velocity of a thermal-electric domain is small to the extent that the thermal emf coefficient α is small. Therefore the situation of greatest interest is where the nonuniform perturbation is also quite small. In the opposite case pinning occurs, that is, the thermal-electric domain is bound to the nonuniformity.

Without significant loss of generality we can allow for the nonuniformity by introducing the term $f_n(T, \varphi)$ on the right-hand side of Eq. (23). For $f_n \ll f$ the thermal-electric domain motion that is established in a time much larger than the characteristic time of an instability can, for any "energy" of the thermal-electric domain, be described by an adiabatic approximation similar to that developed above. If the domain amplitude is not small, then, up to corrections that are small in f_n , the temperature distribution has the form $T(\varphi, t) = \theta(\varphi - \lambda(t), \bar{E}, \bar{j})$, where $\theta(\varphi)$ is the 2π -periodic function that is defined by Eq. (29) or (30) and \bar{E} and \bar{j} are the "energy" of a domain and the domain current that correspond to the given values of U and L . The requirement that the nonuniformity correction to θ be small gives the following differential equation for the phase shift $\lambda(t)$:

$$L \left(\frac{d\lambda}{dt} \right) = s - F(\lambda), \quad F(\lambda) = \frac{1}{B} \left\langle \frac{d\theta}{d\varphi} f_n(\varphi + \lambda(t)) \kappa(\theta) \right\rangle, \quad (52)$$

where B is a number independent of λ and given by

$$B = 2^{1/2} \int_{\varphi_{\min}}^{\varphi_{\max}} C_v(T) [E - W(T, j)]^{1/2} dT,$$

and s is the velocity of a thermal-electric domain under uniform conditions (formula (14)). As can be seen from Eq. (52), when $s > \max F(\lambda)$, nonuniformities do not prevent domain motion, but only change their velocity. If $s < \max F(\lambda)$, then domain pinning at the nonuniformity occurs at the point λ_0 where $F(\lambda_0) = s$ and $dF/d\lambda > 0$.

In the case of small-amplitude domains (and $f_n \ll f$) the analysis is "shortened," as was discussed above, and $T(\varphi, t)$ is determined by formula (43). A small nonuniformity leads to the two terms

$$\begin{aligned} \varepsilon &= (\pi \sqrt{32} \kappa / LC_v) |f_n^{(1)}| \sqrt{VE} \cos \lambda, \\ \omega &= (\pi \sqrt{8} \kappa / LC_v) |f_n^{(1)}| E^{-1/2} \sin \lambda, \end{aligned}$$

on the right-hand sides of Eq. (48) and (49), respectively, where $f_n^{(1)}$ is the first harmonic of the periodic function $f_n(\theta(\varphi), \varphi)$. The "nonuniformity" corrections ε and ω , by mixing the variables $E(t)$ and $\lambda(t)$, can lead not only to thermal-electric domain pinning, but also to a new, self-oscillatory mode, which corresponds to the system going into the limiting cycle. An in-depth analysis of this situation is outside the scope of this paper and will be investigated separately.

APPENDIX I

For small-amplitude domains (see Sec. 2), the differential resistance at the end point j_e has the form

$$\rho_L = U_j'(0, j_e) - \frac{U_E'(0, j_e)}{E_E'(0, j_e)} \frac{dL_{cr}}{dj} \Big|_{j=j_e}. \quad (AI.1)$$

It follows therefore that ρ_L vanishes for at least two values of the current $j = j_{a,b}$. Actually, it follows from (AI.1) that $\rho_L \approx dU_0/dj < 0$ in the neighborhood of current values for which $dL_{cr}/dj = 0$. However, $\rho_L > 0$ in the neighborhood of $j = j_A$ and of $j = j_B$ (see Fig. 1), where $L_c(j) = 2\pi/(-f')^{1/2}$ goes to infinity. It is easy to see that this last relation is true if one notes that, in the zero-order approximation in the parameter $E/W_0 \ll 1$, it follows from (15) and (16) that in the neighborhood of j_A and j_B

$$U_i'(0, j) = j\rho(T_2(j))L_{cr}(j), \quad (AI.2)$$

$$U_E'(0, j) = j\rho(T_2(j))L$$

$$\left[-\frac{5}{24} \frac{(f'')^2}{(f')^3} + \frac{f'''}{8(f')^2} + \frac{\rho' f''}{2\rho(f')^2} \right]_{T=T_2(j)}, \quad (AI.3)$$

$$E_E'(0, j) = L_{cr}(j) \left[-\frac{5}{24} \frac{(f'')^2}{(f')^3} + \frac{f'''}{8(f')^2} \right]_{T=T_2(j)}. \quad (AI.4)$$

Substituting (AI.2)–(AI.4) in (AI.1) and using (1), we find that for values of j close to j_A and j_B , the differential resistance ρ_L is $\rho_L \approx -2Lq'\rho/5f'd > 0$.

APPENDIX II

To express $Q(0)$ (see (35)) in terms of the differential resistance of the dynamic I-V characteristic:

$$\rho_d \equiv \frac{dU_d}{dj} = \langle \rho \rangle \left\{ 1 + \frac{\langle \rho'(\partial\theta/\partial j) \rangle}{\langle \rho \rangle} \right\}, \quad (AII.1)$$

we differentiate Eq. (29) with respect to the current \bar{j} for fixed $\bar{L}(\bar{E}, \bar{j}) = L$:

$$\hat{H}(\kappa \partial\theta/\partial \bar{j}) = 2\bar{j}\rho(\theta). \quad (AII.2)$$

Here \hat{H} is the operator defined by expression (27). It follows from (AII.2) and (32) that the function $\kappa \partial\theta/\partial \bar{j}$ can be written in the form

$$\kappa \frac{\partial\theta}{\partial \bar{j}} = 2\bar{j} \sum_v \frac{\langle \psi_v \rho(\theta) \rangle}{\lambda_v} \psi_v. \quad (AII.3)$$

Substituting (AII.3) into (AII.1) and comparing the resulting

expression with formula (35) evaluated at $p = 0$, we obtain relation (37).

¹⁾We note that even if σ depends only weakly on T , the inequality (2) can hold because of the existence of the decreasing segment of the function $q(T)$. This occurs in the case of cooling the sample in a liquid during the transition from nucleate boiling to film boiling. In this situation, which corresponds, in essence, to the constant current regime, a thermal-electric domain is unstable, and therefore the interpretation given in Ref. 6, that the thermal-electric domains observed by the authors of Refs. 4 and 5 are manifestations of a boiling crisis, is not correct.

¹V. L. Bonch-Bruевич, I. P. Zvyagin, and A. G. Mironov, Domennaya elektricheskaya neustoichivost' v poluprovodnikakh, [Domain Electric Instability in Semiconductors], Nauka, Moscow (1972).

²A. A. Slutskin and A. M. Kadigrobov, Pis'ma Zh. Eksp. Teor. Fiz. **28**, 219 (1978), [JETP Lett. **28**, 201 (1978)].

³A. A. Slutskin, Zh. Eksp. Teor. Fiz. **58**, 1098 (1970), [Sov. Phys. JETP **31**, 589 (1970)].

⁴V. V. Boiko, Yu. F. Podrezov, and N. P. Klimova, Pis'ma Zh. Eksp. Teor. Fiz. **35**, 524 (1982), [JETP Lett. **35**, 649 (1982)].

⁵Yu. N. Tszyan and N. I. Logvinov, Fiz. Nizk. Temp. **8**, 774 (1982), [Sov. J. Low Temp. Phys. **8**, 388 (1982)].

⁶G. I. Abramov, A. Vl. Gurevich, V. M. Dzigutov, R. G. Mints, and L. M. Fisher, Pis'ma Zh. Eksp. Teor. Fiz. **37**, 453 (1983), [JETP Lett. **37**, 535 (1983)].

⁷L. D. Landau and E. M. Lifshitz, Elektrodinamika Sploshnykh Sred, Fizmatiz, Moscow (1959) §25, [Electrodynamics of Continuous Media, Pergamon Press, Oxford (1960)].

⁸V. A. Starodub and I. V. Krivosheĭ, Uspekhi Khimii **51**, 764 (1982).

⁹M. A. Lavrent'ev and L. A. Lyusternik, Kurs Variatsionnogo Ischisleniya, [Course in Variational Calculus], Gostekhizdat, Moscow (1950), Ch. IX; [R. Courant and D. Hilbert, Methods of Mathematical Physics, Vol. 1. Chap VI, 2 vols., Wiley, New York 1953.]

Translated by J. R. Anderson